Proceedings of ASME Turbo Expo 2004
Power for Land, Sea, and Air
14-17 June 2004, Vienna, Austria

Paper Number GT2004-54254

SCREENING AND EVALUATION OF MATERIALS FOR MICROTURBINE RECUPERATORS

Edgar Lara-Curzio, R. Trejo, K. L. More, P. A. Maziasz and B. A. Pint
Metals & Ceramics Division
Oak Ridge National Laboratory
Oak Ridge, TN 37831-6069

ABSTRACT

The effects of stress, temperature and exposure to microturbine exhaust gases on the mechanical properties and corrosion resistance of candidate materials for microturbine recuperators were investigated. Results are presented for 347 stainless steel metallic foils after 500-hr exposure to temperatures between 620°C and 760°C at a tensile stress of 50 MPa. It was found that the material experienced accelerated attack at the highest temperature and that the corrosion products consisted of mixed oxides of iron and chromium. It was also found that exposure at the highest temperatures resulted in significant decrease in both tensile strength and ductility. ORNL's microturbine recuperator test facility, where the exposures were carried out, is also described.

INTRODUCTION

The challenging performance targets for the next generation of microturbines include fuel-to-electricity efficiency of 40%, capital costs less than $500/kW, NOx emissions reduced to single parts per million, several years of operation between overhauls, life of 40,000 hours and fuel flexibility [1]. It is clear that significant increases in microturbine efficiency can be achieved by increasing engine-operating temperatures, and that this can only be realized through the use of advanced metallic alloys and ceramics for high-temperature components.

One of the critical components in low-compression ratio microturbines is the recuperator, which is responsible for a significant fraction of the overall efficiency of the microturbine [2]. Conventional recuperators are thin-sheet metallic heat exchangers that recover some of the waste heat from the exhaust stream and transfer it to the incoming air stream. The preheated incoming air is then used for combustion because less fuel is required to raise its temperature to the required level at the turbine inlet. Most of today's compact recuperators are manufactured using 300 series (e.g.- 347) stainless steels which are used at exhaust-gas temperatures below about 650° C [3]. At higher temperatures, these materials are susceptible to creep deformation and oxidation, which lead to structural deterioration and leaks, reducing the effectiveness and life of the recuperator. The temperature requirements for the next generation of microturbines have prompted efforts to screen and evaluate candidate materials with the required creep and corrosion resistance. Furthermore, developmental efforts will be needed to adapt current recuperator manufacturing processes to advanced alloys, to reduce costs, and enable long-term reliable operation at higher temperatures.

As part of a program sponsored by the U.S. Department of Energy to support microturbine manufacturers in the development of the next generation of microturbines, a recuperator test facility was established at Oak Ridge National Laboratory (ORNL). The objective of this test facility is to screen and evaluate candidate materials for microturbine recuperators under stress at turbine exit temperatures as high as 850°C inside a microturbine. Furthermore, the preparation of samples for these experiments, which requires welding test specimens to a sample holder, provides the means for

identifying potential manufacturability barriers with a particular material.

In this paper the results from the evaluation of 89-μm (3.5 mils) thick foils of 347 stainless steel after 500 hrs of exposure in ORNL's microturbine recuperator testing facility at turbine exit temperatures as high as 785°C is reported. The effect of exposure on the corrosion resistance and tensile strength and ductility and of the material is discussed. The operation of the test facility and current work are also discussed.

NOMENCLATURE

cm	centimeter
kW	kilowatt
mm	millimeter
ORNL	Oak Ridge National Laboratory
psi	pound per square inch.
TET	turbine exit temperature
TIT	turbine inlet temperature

EXPERIMENTAL

In 2001, ORNL acquired a 60kW Capstone microturbine. In collaboration with Capstone Turbine Corp., the microturbine had been modified to achieve higher TET values. The system also had been modified by the incorporation of six port bosses to allow the placement of test specimens at the entrance of the recuperator. Figure 1 shows a photograph of ORNL's microturbine recuperator testing facility and a schematic of the modified 60 kW microturbine indicating the location of the port bosses with respect to the location of the radial recuperator.

The sample holders are cylindrical in shape and allow the placement of four test specimens. Figure 2 shows a photograph of sample holders with and without foil test specimens. The sample holders have orifices to allow the placement of thermocouples to monitor the temperature of each metallic foil specimen during the test. These orifices also allow the pressurization of the sample holder with a gas (e.g.- air), which in turns allows the mechanical stressing of the test foils. This is an important feature of this test facility because it allows the simultaneous investigation of the effects of temperature, stress and environment on the durability of candidate materials.

For the results reported in this paper, four 0.089-mm thick, 75-mm long and 14-mm wide strips of 347 stainless steel foils were laser-welded onto a 347 stainless-steel sample holder. The diameter of the sample holder onto which the foils were welded was 23.1 mm. Prior to welding the foils, type-K thermocouples were placed in each one of the four holes in the sample holder. Sample holders are fabricated using the same material being evaluated to avoid subjecting the foil specimens to undesirable stresses due to mismatch in thermal expansion. To date, 347 stainless steel foils have been welded effectively to stainless steel sample holders by both laser and e-beam welding. One advantage of the methodology developed to screen and evaluate candidate materials for the next generation of microturbine recuperators is that it can identify potential manufacturability problems, such as lack of weldability of the material.

After the metallic foils are welded to the sample holder, and the sample holder is checked for leaks, the latter is inserted into the microturbine through one of the port bosses as illustrated in Figure 3. The sample holder is connected to a water-cooled block to protect the pressure transducer and the thermocouple seals that permit the pressurization of the sample holder, from high-temperature exposure. ORNL's microturbine recuperator test facility includes a pressure control system to maintain a constant value of the pressure inside the sample holder. The pressure control system includes a pressure transducer, a pressure regulator, a pressure controller and a solenoid valve. Whenever the value of the pressure inside the sample holder drops below the set point, the pressure controller actuates a solenoid valve to equilibrate the pressure inside the sample holder with the pressure set by the pressure regulator. By maintaining a continuous record of the gas pressure inside the sample holder during the test it is possible to know if the foil test specimens experience creep deformation, because the volume of the sample holder would increase resulting in a pressure drop. Also, the pressure control system would indicate whenever a leak has occurred, which would be indicative of failure of the foil. For the results reported in this paper, the sample holder was pressurized using air at 60 psi, which is the pressure of the compressed air in a C60 Capstone microturbine.

During regular operation, sample holders are subjected to a temperature gradient as illustrated by the temperature profile in Figure 4. The profile shown in Figure 4 is for a nominal TET value of 800°C. For this case the temperature variation along the length of the sample holder spans between 650°C and 760°C. The temperature gradient results from the configuration of the microturbine and it turns out a nice feature of this test facility because it allows for the evaluation of materials over a wide range of temperatures during the same test.

Prior to the exposure tests in the microturbine, the baseline mechanical properties of the 347 stainless steel foils were determined. Miniature dog-bone shaped tensile specimens were obtained by electron discharge machining from foils 20.3 cm wide and 0.089 mm thick. Test specimens were obtained with their main axis either parallel or perpendicular to the rolling direction. The dimensions of the dog-bone shaped miniature tensile specimens were 10 mm long, with a gauge section 1.27-mm wide and 3.8-mm long. The tensile stress-strain behavior of the miniature test specimens was determined under a constant crosshead displacement rate of 0.01 mm/min using an electromechanical testing machine. A special set of grips and alignment fixture were used to transfer the load to the test specimens and to ensure alignment to eliminate spurious bending strains. Because of the small dimensions of the test specimens it was not possible to determine the strain directly. However, the tensile strain of the test specimens was estimated after correcting the recorded crosshead displacement from the contribution of the machine compliance to the recorded displacement. Values for the 0.2% yield stress, ultimate tensile strength and strain failure were obtained from each stress-strain curve.

At the end of a 500-hr test exposure the sample holder was retrieved from the microturbine, and the foils were removed from the sample holder. Miniature tensile test specimens were obtained from the foils along with samples for microstructural

characterization using electron microscopy and chemical analysis using an electron microprobe. Table I summarizes the settings for the test.

RESULTS AND DISCUSSION

Figure 5 presents a collection of tensile stress-strain curves obtained from the evaluation of miniature dog-bone specimens of as-received 347 stainless steel foils. As indicated by the inset in the graph, the test specimens were obtained with their axis parallel to the foil rolling direction. The evaluation of test specimens with their axis perpendicular to the rolling direction produced tensile strength and ductility values that were found to be significantly different, at the 95% confidence level, than those obtained from the evaluation of test specimens aligned parallel to the rolling direction. These results are summarized in Table II. The fracture surfaces of these test specimens revealed features that are typical of ductile failure and fracture planes were found to be aligned at 45° with respect to the loading direction, as illustrated in Figure 6. This orientation of the fracture plane is consistent with the large amount of deformation experienced by the test specimens and the alignment of the high-density planes parallel to the direction of maximum shear stress.

During the test the temperature of each test specimen, which was monitored using type-K thermocouples, was recorded and it is plotted in Figure 7 for the 500-hr test duration. These values of temperature are consistent with the temperature profile presented in Figure 4, which had been obtained by positioning a type-K thermocouple at 5 mm intervals along a sample holder during microturbine operation at TET=800°C.

At the end of the test, the pressure was released from the sample holder and the sample holder was allowed to cool down. After the sample holder was removed from the microturbine it was found to be heavily corroded as illustrated in Figures 8 and 9. The photograph in Figure 9 is a close-up of foil A, which had experienced the highest temperature during the test. The photograph in Figure 8 also shows that the foil in location A had ballooned as a result of creep deformation. It was also found that this foil had cracked in a direction parallel to the axis of symmetry of the sample holder.

The foils were removed from the sample holder, and miniature test specimens were obtained by electric discharge machining, as illustrated in Figure 10. A total of fourteen test specimens were obtained from each foil, except from foil A, where only six test specimens were obtained due to high degree of damage in the material.

Figures 11 and 12 show a collection of stress-strain curves obtained from the tensile evaluation of miniature tensile specimens obtained from foils A and D, respectively. When comparing these results with those shown in Figure 5 for the as-processed 347 stainless steel foils, it can be observed that both the tensile strength and ductility of test specimens obtained from foil A have been significantly affected after the 500-hr test exposure. Although the ultimate tensile strength of test specimens obtained from foil D was not affected, it was found that the ductility had decreased. Loss of ductility in this material usually results from carbide precipitation between 400°C and 800°C. Table III summarizes the results from the evaluation of miniature tensile specimens from foils A to D and the strength results, normalized to the as-received values are plotted in Figure 13. Analysis of the fracture surfaces of the miniature tensile specimens revealed features that are associated with ductile failure, even by the remaining base metal in foil A. Figures 14 and 15 contain scanning electron micrographs of fracture surfaces of miniature tensile specimens obtained from foils A and B, respectively.

The microstructure and the chemical composition of the corrosion products that formed on the 347 stainless steel foils were examined using electron microscopy and electron microprobe analysis. Figure 16 is a composite containing micrographs of the cross-section of foils A to D after 500-hr exposure in ORNL's microturbine at a nominal TET of 800°C.

This composite clearly illustrates the effect of temperature on the corrosion resistance of the material. It can be observed that the thickness of the oxide layer that formed on the surface of the foils that was exposed to the microturbine exhaust stream increased with temperature and was more than 20-μm thick on foil A. The micrographs also illustrate the asymmetry in the thickness and nature of the oxidation products between the surface that was exposed to the exhaust side and the surface that was exposed to compressed air inside the sample holder. It is believed that this asymmetry in the corrosion resistance of the material results from the high concentration of water vapor in the microturbine exhaust gases. While the effect of water vapor is currently the focus of significant research, there is still no widely accepted mechanism for its role in reducing the corrosion resistance of chromia-forming stainless steels [5].

The chemical composition of the oxidation products was determined using an electron microprobe. Figure 17 shows elemental maps for iron, chromium, nickel, oxygen and niobium for a region from a cross-section of foil A. It was found that the oxidation products that formed on the surface of Foil A that was exposed to the microturbine exhaust gases consisted of layered oxides of chromium, nickel and iron. The oxide layer closest to the metallic substrate consists mainly of oxides of nickel and chromium, whereas the outermost oxidation layer is primarily comprised of oxides of iron. The elemental maps also revealed that the interface between the metallic substrate and the first oxidation layer was predominantly rich in chromium. The concentration maps showed that the grain boundaries in the base metal are depleted of chromium, which is consistent with mechanisms that have been proposed to explain the kinetics of formation of the oxide layers [5]. One hypothesis is that accelerated attack occurs after the chromium content becomes depleted at the metal-scale interface below some critical level, which is dependent on the other elements in the alloy such as Ni. The presence of water vapor in the microturbine exhaust gas stream leads to faster scale growth and increased evaporation of Cr_2O_3 from the scale as $CrO_2(OH)_2$ [5]. These two processes lead to an increased consumption rate of chromium in the metal compared to oxidation in dry air. Because the diffusion rate of chromium in the metal is not fast enough compared to the consumption rate, a chromium depleted region forms in the metal near the surface. After some incubation time nodules of FeO_x begin to form. Whether the nodules form due to the chromium depletion in the metal or some other mechanism has not been determined.

Although the amount of oxidation on the surface of foils exposed to compressed air inside the sample holder was much less than that on the surface exposed to the microturbine exhaust gases, there is evidence that in Foil A there exists a layer of chromium oxide and iron oxide nodules, that might be indicative of the onset of accelerated attack. Although the concentration of water vapor in compressed plant air, which was used to pressurize the sample holder at 60 psi, is much less than that in the microturbine exhaust stream, it is likely that the concentration of water vapor might be sufficient to explain the formation of the iron oxide nodules and depletion of chromium from the grain boundaries in the base metal.

WORK IN PROGRESS

Currently, the following alloys are being evaluated in ORNL's microturbine test facility: Haynes 120®, Haynes 214®, Haynes 230® and modified 347 stainless steels.

SUMMARY

A test facility for screening and evaluating candidate materials for the next generation of microturbine recuperators has been designed and is operational at Oak Ridge National Laboratory. The core of the test facility is a 60kW Capstone microturbine, which was modified to operate at higher turbine exit temperatures and to allow the placement of test specimens at the entrance of its radial recuperator. Sample holders have been designed and instrumented to allow for the continuous recording of the temperature of the thin metallic foil test specimens and to subject these to mechanical stresses through the internal pressurization of the sample holder. Materials under evaluation are welded to the sample holder using laser or e-beam techniques and allow for the identification of potential manufacturability showstoppers.

Results have been presented from the evaluation of 89-μm thick foils of 347 stainless steel after 500-hr exposure at a turbine exit temperature of 800°C and a tensile stress of 50 MPa, which results from pressurizing the sample holder at 60 psi. It was found that material retained 85% of its strength for exposure temperatures up to 700°C, but test specimens subjected at 760°C experienced creep deformation and a significant decrease in tensile strength and ductility. It was also found that the thickness of the oxide products increased with exposure temperature and that test specimens subjected at 760°C experienced accelerated attack. The oxidation products consisted of two layers: the layer closest to the base metal contained mixed oxides of nickel and chromium, whereas the outermost layer consisted solely of iron oxides. Although the oxide layers that formed on the surface of the test specimens exposed to the microturbine exhaust gases were thicker than those that formed on the surface exposed to compressed air inside the sample holder, there was evidence of the formation of iron-rich oxide nodules on the latter.

Ongoing work is focused on the evaluation of candidate alloys (e.g.- Haynes 120®, Haynes 214®, Haynes 230® and modified 347 stainless steels) for the manufacture of the next generation of microturbine recuperators.

ACKNOWLEDGMENTS

Research sponsored by the U.S. Department of Energy, Assistant Secretary for Energy Efficiency and Renewable Energy, Distributed Energy Resources, as part of the Microturbine Materials Program, under contract DE-AC05-00OR22725 with UT-Battelle, LLC. The contributions from Mr. Randy Parten in are greatly appreciated. The authors are indebted to Matt Stewart of Capstone Turbine for providing the materials using in this study.

REFERENCES

1. "Advanced Microturbine Systems Program, Plan For Fiscal Years 2000 Through 2006," U.S. Department of Energy, Office of Energy Efficiency and Renewable Energy, Office of Power Technologies. March 2000.
2. C. F. McDonald, "Heat Recovery Exchanger Technology for Very Small Gas Turbines," Intl. Journal of Turbo and Jet Engines," vol. 13 (1966) pp. 239-261.
3. O. O. Omatete, P. J. Maziasz, B. A. Pint, and D. P. Stinton, "Assessment of Recuperator Materials for Microturbines," ORNL/TM-2000-304.
4. Lara-Curzio, E., Maziasz, P. J., Pint, B. A., Stewart, M., Hamrin, D., Lipovich, N. and DeMore, D., 2002, "Test Facility for Screening and Evaluating Candidate Materials for Advanced Microturbine Recuperators," ASME Paper #2002-GT-30581, presented at the International Gas Turbine & Aeroengine Congress & Exhibition, Amsterdam, Netherlands, June 3-6, 2002.
5. B. A. Pint and K. L. More, "Stainless Steels with Improved Oxidation Resistance for Recuperators," Proceedings of ASME Turbo Expo 2004, Paper GT2004-53627, 14-17 June 2004, Vienna, Austria.

Table I. Microturbine settings for 500-hr test.

Engine Speed	45,000 RPM
Turbine Exit Temperature	800°C
Sample holder pressure	60 psi
Fuel	natural gas

Table II. Summary of tensile results for as-processed materials.

347 Stainless Steel	0.2% Yield Strength (MPa)	Ultimate Tensile Strength (MPa)	Strain at Failure (%)
⊥ to rolling direction	384 ± 33	717 ± 7	78 ± 5
∥ to rolling direction	379 ± 16	766 ± 8	66 ± 1

Table III. Summary of tensile properties of 0.089-mm thick foils of 347 stainless steel after 500-hr test at a TET of 800°C and tensile tangential stress of 50 MPa.

Foil	0.2% Yield Strength (MPa)	Ultimate Tensile Strength (MPa)	Failure strain (%)
A	310	351	4.9 ± 1.8
B	391	576	33 ± 6.6
C	410	647	35 ± 1.2
D	371	645	36 ± 2.8

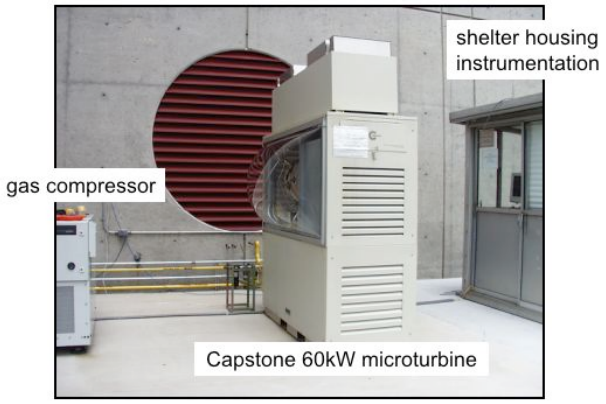

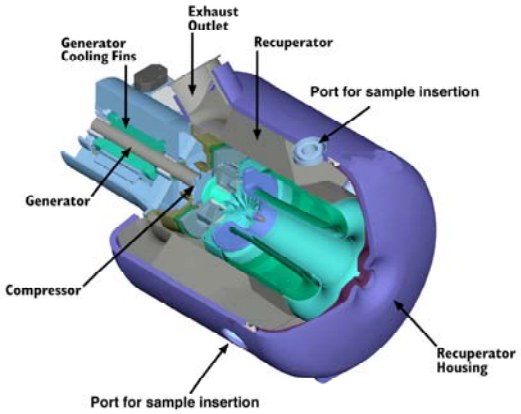

Figure 1. (a) ORNL's microturbine recuperator testing facility. (b) Schematic of modified 60kW Capstone microturbine. Note location of port bosses for placement of test specimens at the entrance of the radial recuperator.

Figure 2. Sample holders with and without foils. The holes in the sample holder allow the placement of thermocouples and the flow of gas for mechanically stressing the foils through the internal pressurization of the sample holder.

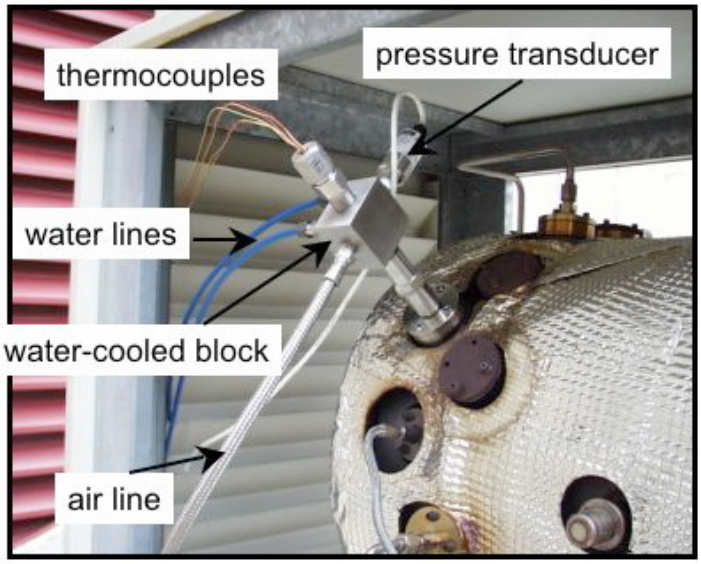

Figure 3. ORNL's microturbine recuperator testing facility indicating the placement of test specimens.

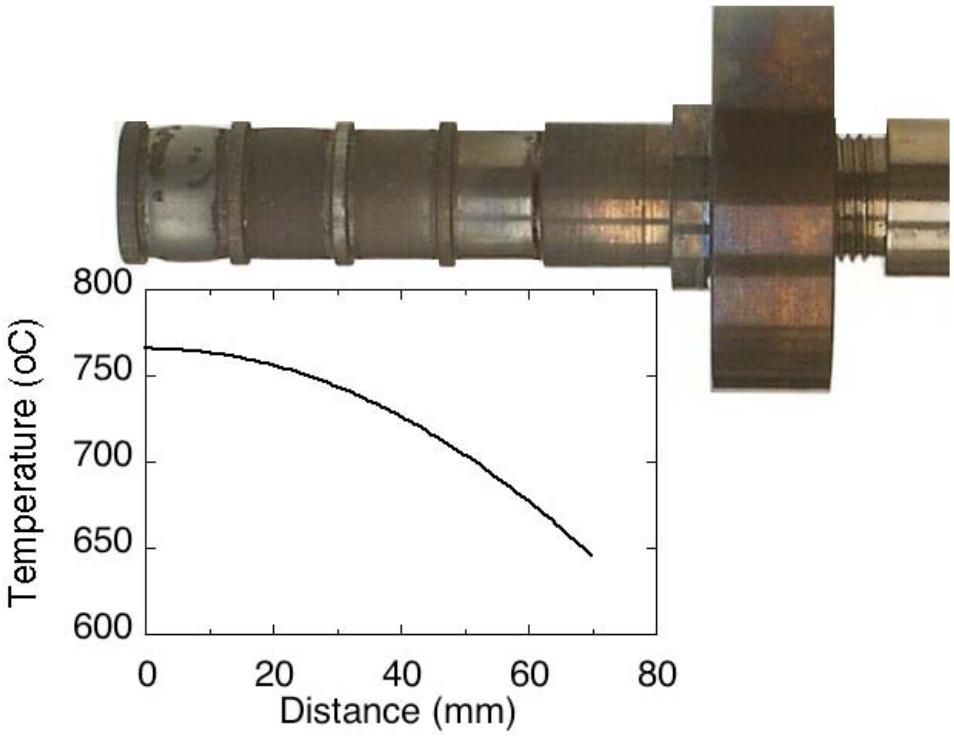

Figure 4. Temperature distribution along stainless sample holder for TET=800°C.

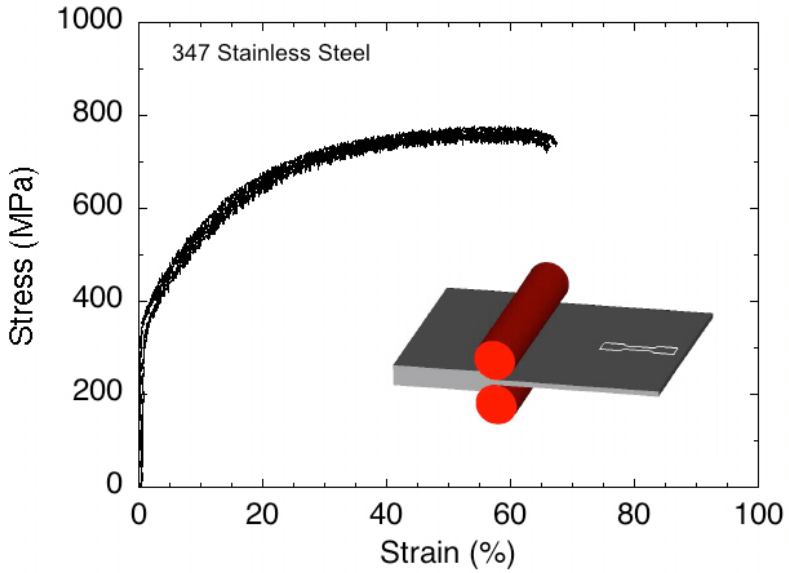

Figure 5. Stress-strain curves obtained from the tensile evaluation of miniature dog-bone shaped test specimens of 347 stainless steel 0.089-mm thick foils. Test specimens had been obtained by electric discharge machining with their axis parallel to the foil rolling direction.

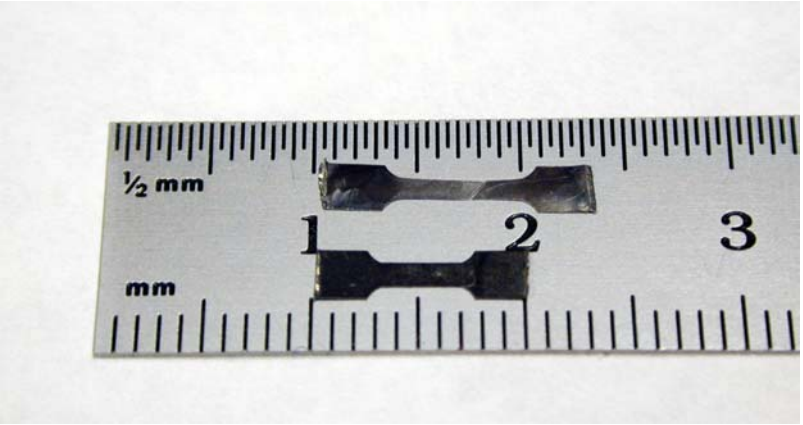

Figure 6. Optical micrograph of as-processed 347 stainless steel after tensile evaluation at ambient conditions. Note that the tested specimen has experienced significant plastic deformation and that its fracture plane is aligned at 45° with respect to the loading direction.

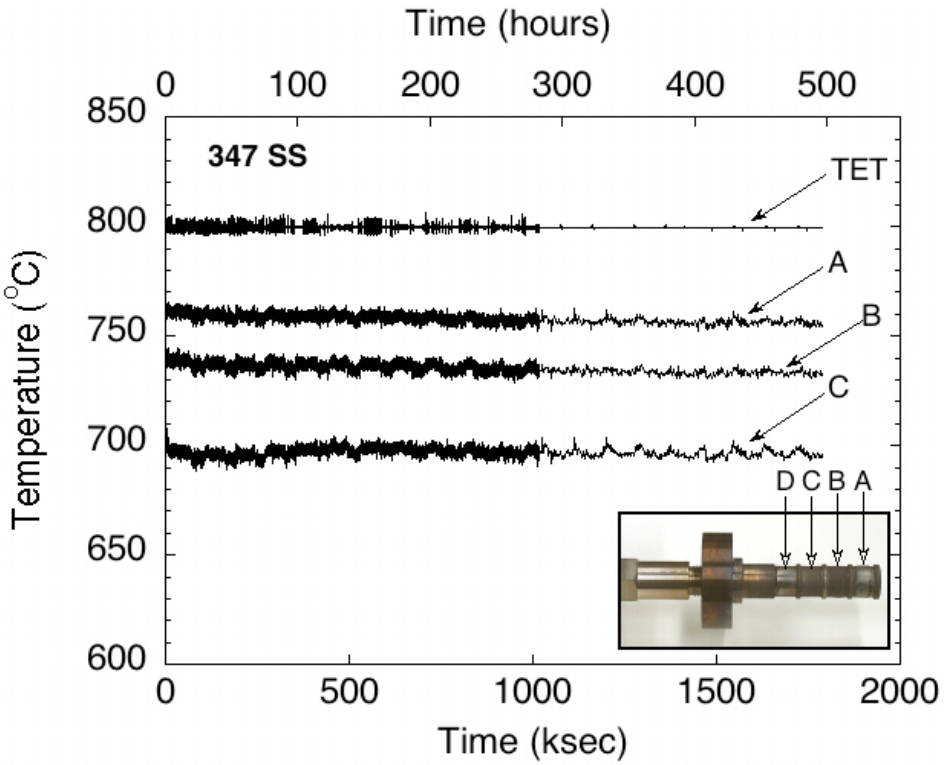

Figure 7. Temperature history for 500-hr test to evaluate the behavior of 0.089-mm thick foils of 347 stainless steel.

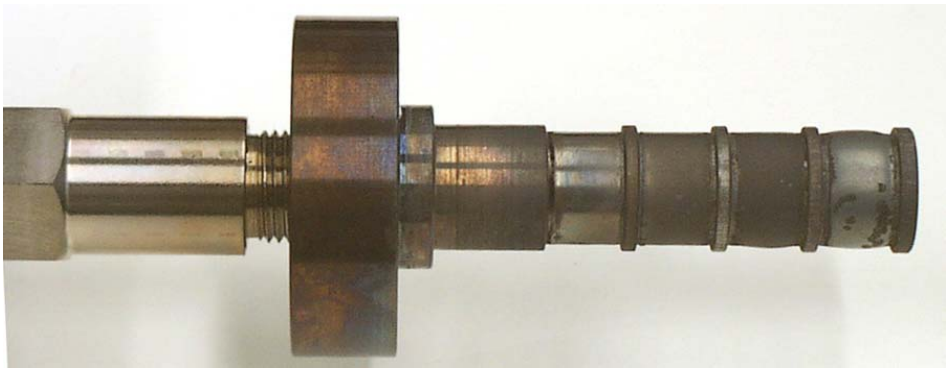

Figure 8. Optical micrograph of sample holder with of 0.089-mm thick foils of 347 stainless steel after 500-hr test at TET=800°C and tensile tangential stress of 50 MPa. Note the ballooning of foil A due to creep deformation and the scale on the surface of the foils.

Figure 9. Optical micrograph of foils A and B (0.089-mm thick foils of 347 stainless steel), after 500-hr test at a TET of 800°C and tensile tangential stress of 50 MPa. Note the corrosion scale on the surface of the foils. The weld seam in foil B is evident.

Figure 10. Foil after being removed from sample holder at end of 500-hr exposure test. Fourteen miniature tensile specimens were obtained from each foil.

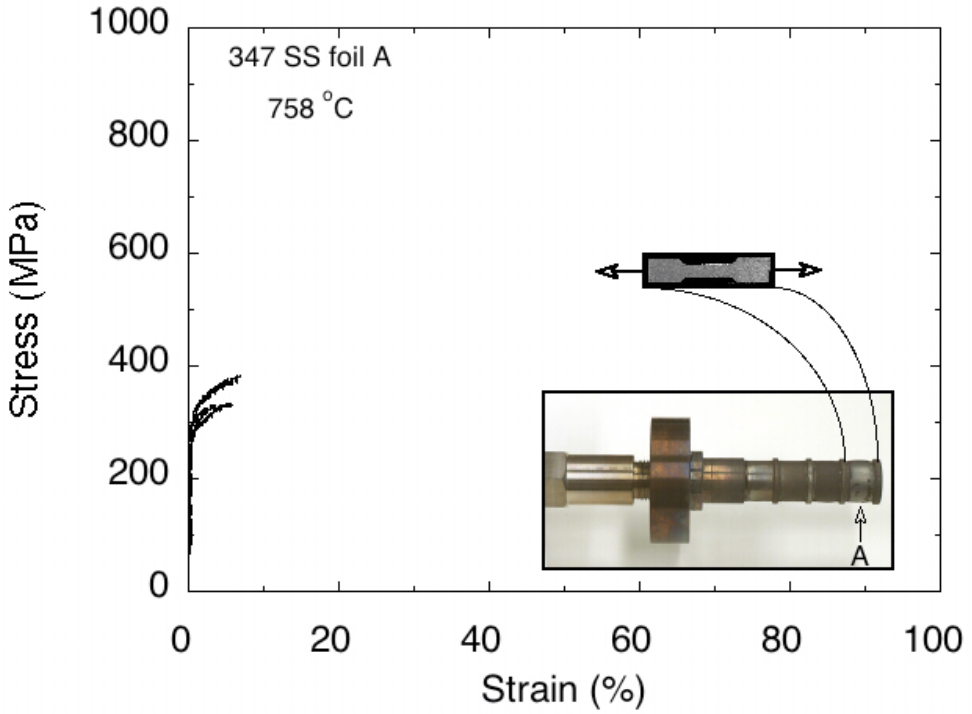

Figure 11. Stress-strain curves obtained from the tensile evaluation of miniature test specimens obtained from foil A (0.089-mm thick foil of 347 stainless steel) after 500-hr test.

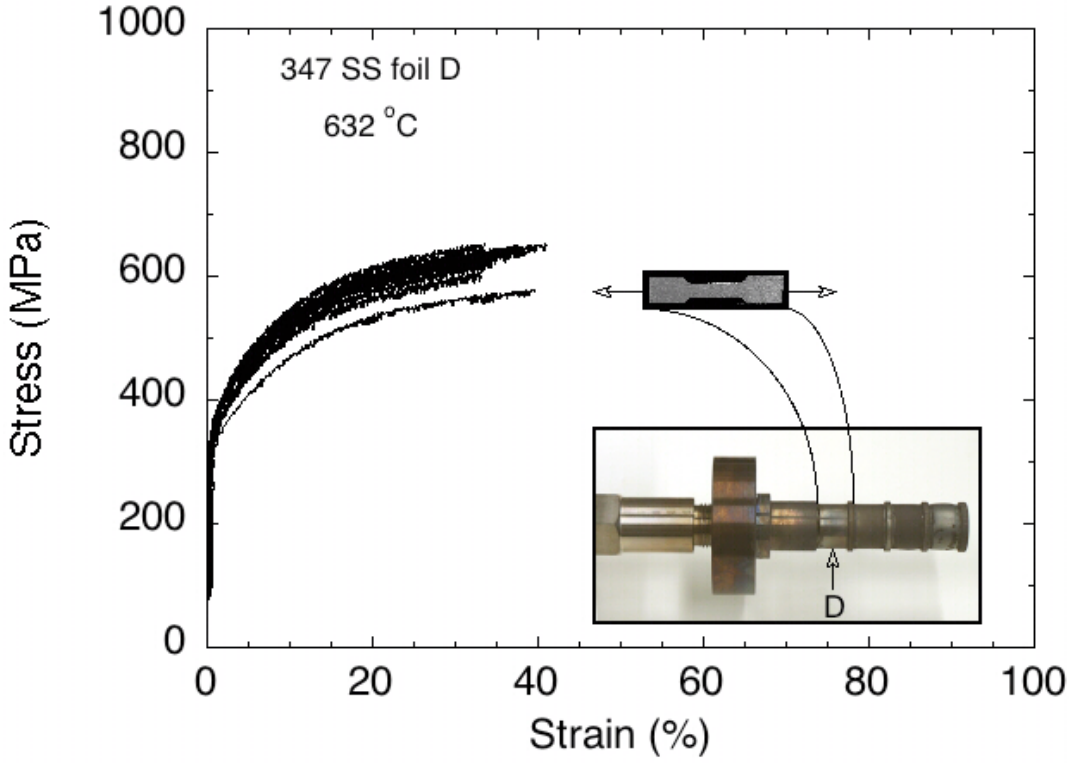

Figure 12. Stress-strain curves obtained from the tensile evaluation of miniature test specimens obtained from foil D (0.089-mm thick foil of 347 stainless steel) after 500-hr test.

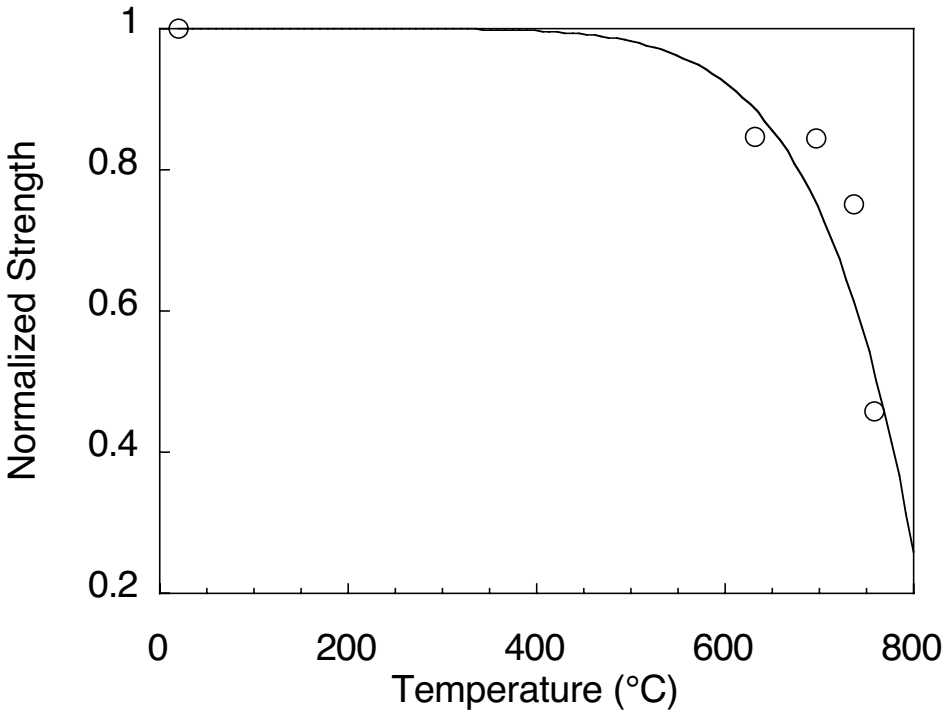

Figure 13. Normalized tensile strength of 0.089-mm thick foils of 347 stainless steel after 500-hr test.

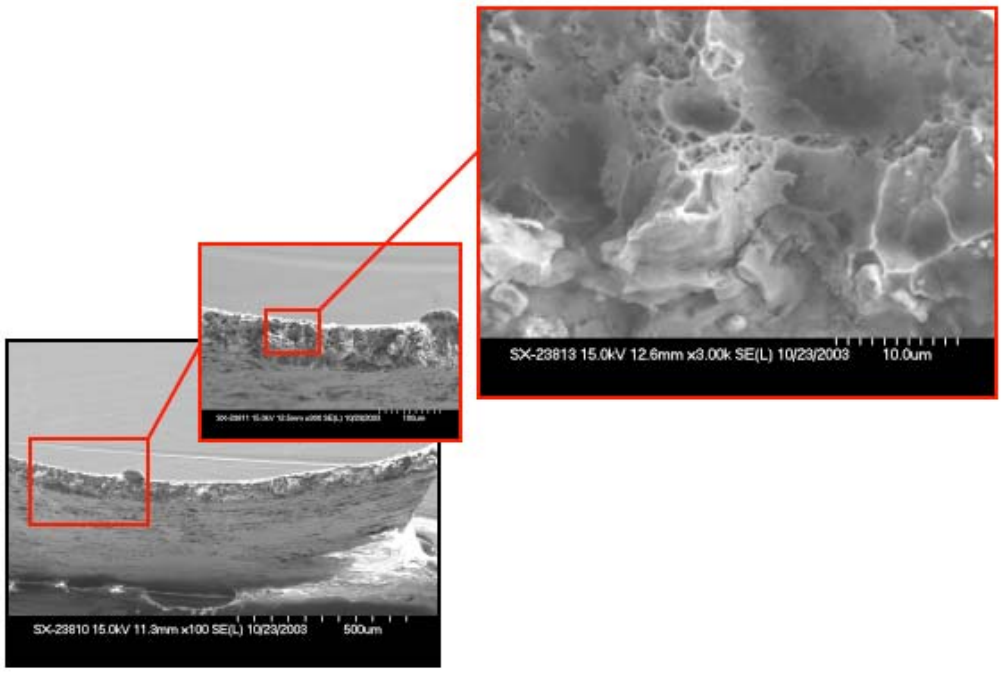

Figure 14. Scanning electron micrograph of fracture surface of foil A after 500-hr tests at 735°C and a tensile stress of 50 MPa. Although the material had experienced extensive corrosion, the base metal still exhibited ductile behavior.

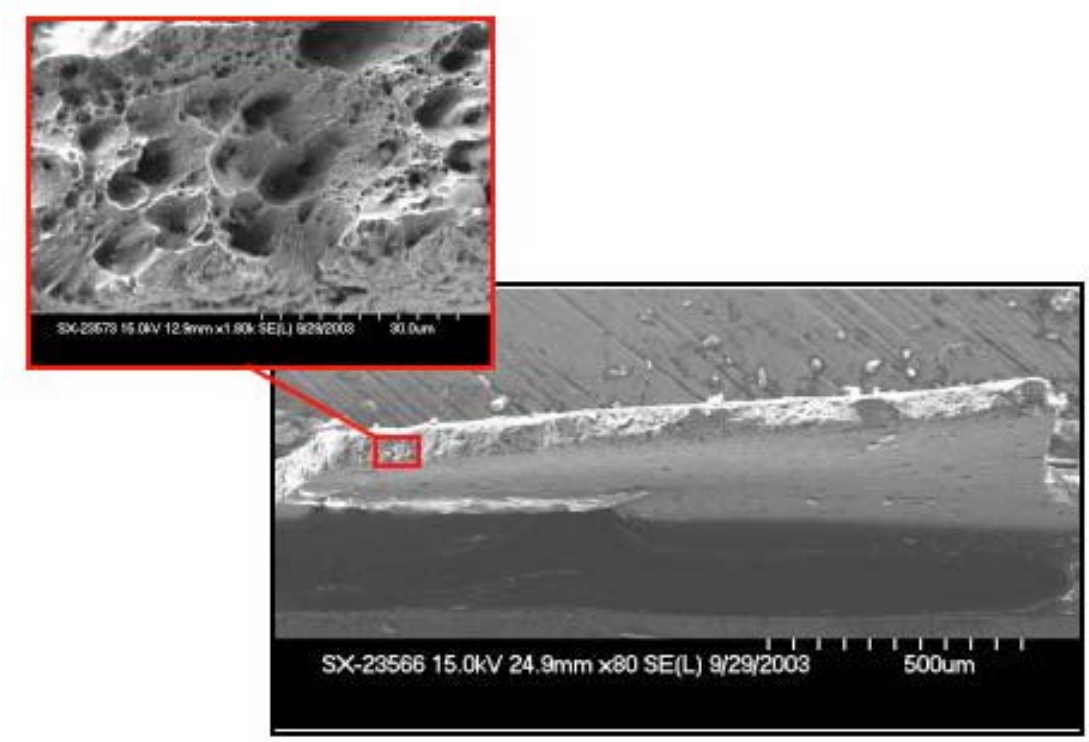

Figure 15. Scanning electron micrograph of fracture surface of foil B after 500-hr tests at 735°C and a tensile stress of 50 MPa.

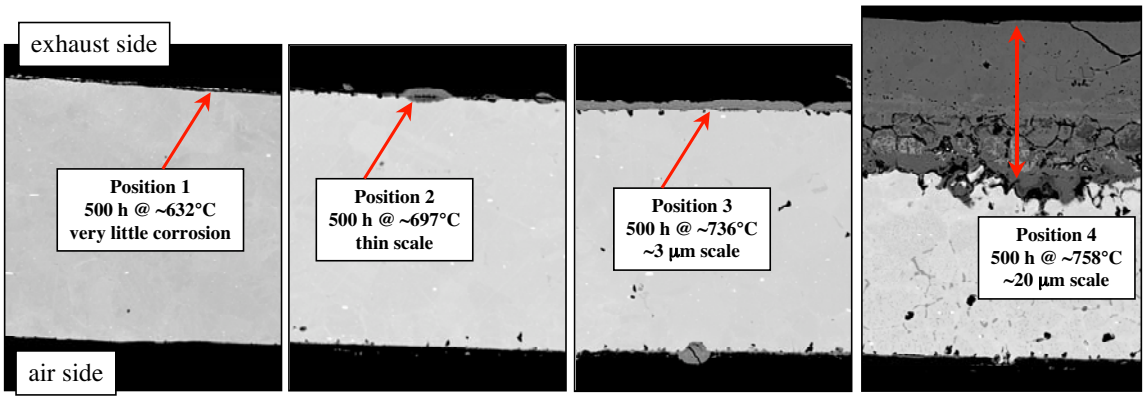

Figure 16. Scanning electron micrographs of cross-sectional areas of 0.089-mm thick foil of 347 stainless steel) after 500-hr test.

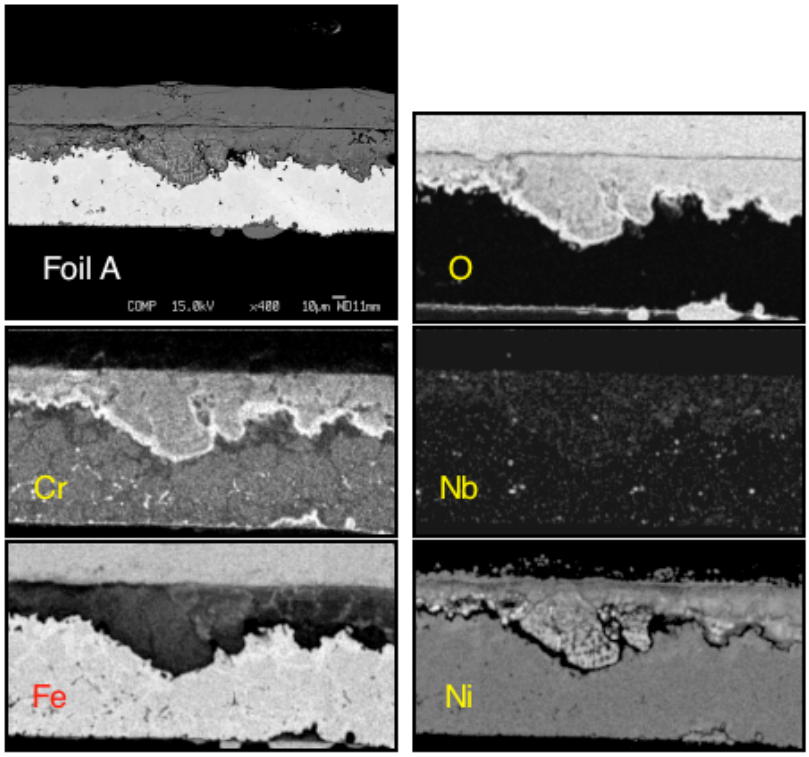

Figure 17. Elemental maps for cross-sectional area of Foil A after 500-hr test.